Magnetic field dependence of the circular dichroism in EuTe

2007 J. Phys.: Condens. Matter 19 406234

(http://iopscience.iop.org/0953-8984/19/40/406234)

IOP PUBLISHING JOURNAL OF PHYSICS: CONDENSED MATTER

J. Phys.: Condens. Matter **19** (2007) 406234 (11pp) doi:10.1088/0953-8984/19/40/406234

Magnetic field dependence of the circular dichroism in EuTe

A B Henriques[1], G D Galgano[1], B L Díaz[2], P H O Rappl[2] and E Abramof[2]

[1] Instituto de Física, Universidade de São Paulo, Caixa Postal 66318, 05315-970 São Paulo, Brazil
[2] LAS-INPE, Avenida dos Astronautas, 1758-Jd. Granja, 12227-010, São José dos Campos, Brazil

Received 1 August 2007, in final form 20 August 2007
Published 21 September 2007
Online at stacks.iop.org/JPhysCM/19/406234

Abstract

The absorption magnetic circular dichroism in EuTe was investigated as a function of the magnetic field at $T = 2$ K. In order to describe the optical spectra theoretically, we developed a model that takes into account the magnetic order of the lattice as a function of the magnetic field. The model allows us to calculate the absorption spectrum as a continuous function of the magnetic field intensity. The theory accounts for the strongly dichroic absorption seen at high fields, and for its continuous evolution towards the $B = 0$ spectrum, which is described by a much weaker and much broader absorption line. The drastic changes observed in the experimental spectra as a function of magnetic field are fully explained by the dependence of the Eu^{2+} spin arrangement on the external magnetic field.

1. Introduction

Magnetic semiconductors are important materials for novel devices based on electronic spin control [1]. In the quest for adequate materials [2] researchers look for systems with a long spin dephasing time for applications in information processing [3], or materials in which the conduction electrons with spins up and down differ greatly in energy for applications in spin-filtering devices [4]. Europium chalcogenides (EuX, X = O, S, Se, Te) are magnetic semiconductors with a wide gap (2 eV), whose magnetism arises from the large magnetic moment, $S = 7/2$, of the Eu atoms in the lattice, which have attracted continuous interest for device applications ever since their discovery in the early 1960s. Polarization control of the lattice spin in EuX can be employed in classical magneto-optical devices [5] and more recently in quantum spin-filters [6].

A prerequisite for the employment of a given material in spintronic devices is a good understanding of its electronic structure. The energy band edges of semiconductors are responsible for their most fundamental characteristics, including the magneto-optical response of the material. To describe the optical properties of EuX, various energy level schemes have been proposed [7–10]. The accepted picture is that the localized $4f^8(^7S_{7/2})$ orbitals at the

Eu^{2+} sites constitute a valence level, whereas the lowest energy conduction band is built from crystal field split $5d(t_{2g})$ states. The gross magneto-optical properties, such as Faraday rotation and optical absorption, can be well described in the framework of the $4f^7(^8S_{7/2}) \rightarrow 5d(t_{2g})$ model. However, no model has yet been successful in describing the absorption edge in detail (for a discussion see [7, 8, 11]) and, although an old problem, a full understanding of the absorption edge is still lacking. Recently, we investigated the band-edge in EuTe and EuSe in high magnetic fields, when the Eu^{2+} spins were ordered ferromagnetically [12]. We discovered a doublet of hugely dichroic narrow lines (splitting 200 meV), and all observations could be well described quantitatively in the framework of the $4f^7(^8S_{7/2}) \rightarrow 5d(t_{2g})$ model. However, the zero-field spectrum was much weaker and showed only a broad absorption band with no resolved features. This could not be understood within the framework of the simple $4f^7(^8S_{7/2}) \rightarrow 5d(t_{2g})$ picture. As a tentative explanation for the drastic difference between the high-field and zero-field spectra, it was speculated that it could be associated with a large dependence of the oscillator strength on the magnetic field, due to the formation of excitons [12]. However, subsequent studies showed that the absorption spectrum changes are too large to be explained by electron–hole correlation effects only [13, 14].

In this paper, we clarify this point; i.e., we demonstrate that the large difference between the zero-field and the high-field absorption spectrum can be fully explained by the changes in the magnetic order of the Eu^{2+} spins as a function of magnetic field. We examine the absorption spectra in the continuous range of fields that lead from antiferromagnetic to ferromagnetic arrangement of Eu^{2+} spins. The orientation of the spins, as a function of the magnetic field, was deduced using the molecular-field model [15], and the well known anisotropy potential for EuTe [16]. At zero field, due to symmetry, the minimum energy state is degenerate, and the sample is broken into a multiple domain structure. The interaction of light with this magnetic field-dependent domain ensemble was examined in the framework of the same $4f^7(^8S_{7/2}) \rightarrow 5d(t_{2g})$ model as used by us previously to describe the interaction of light with a single spin domain [12]; however, in the present investigation the model had to be extended to incorporate the much more complex scenario of multiple canted domains. The calculated absorption spectra are compared to the experimental ones in the whole magnetic field interval—ranging from zero, when the spin order is antiferromagnetic, going through intermediate magnetic fields, when the Eu^{2+} spins are canted, and reaching the high magnetic field region, when complete ferromagnetic order is imposed—and show good agreement within an energy interval of approximately 400 meV at the band-edge.

2. Experimental details

The samples were grown by molecular beam epitaxy on (111) BaF_2 substrates. The thickness of the EuTe epitaxial layer was about 0.2 μm, which allows us to avoid Fabry–Perot interference fringes, which pollute the absorption spectrum of thicker samples [17]. Details of the sample growth are given in [12].

Transmission measurements were performed in the Faraday configuration, using a tungsten light source. The light source was coupled to a monochromator, and the monochromatic light was launched into an optical fiber. The optical fiber conducted light into the interior of a cryostat containing a superconducting coil, within which the sample was cooled to $T = 2$ K. The light output of the optical fiber was collimated by a graded refractive index lens, went through a right-hand circular polarizer, then went through the sample, and was collected by a biconvex lens coupled to a collecting optical fiber, whose output was fed into a photomultiplier tube. The experimental setup is shown schematically in figure 1(a). A detailed drawing of the sample holder tip is shown in figure 1(b). For secure handling of the optical fibers and their

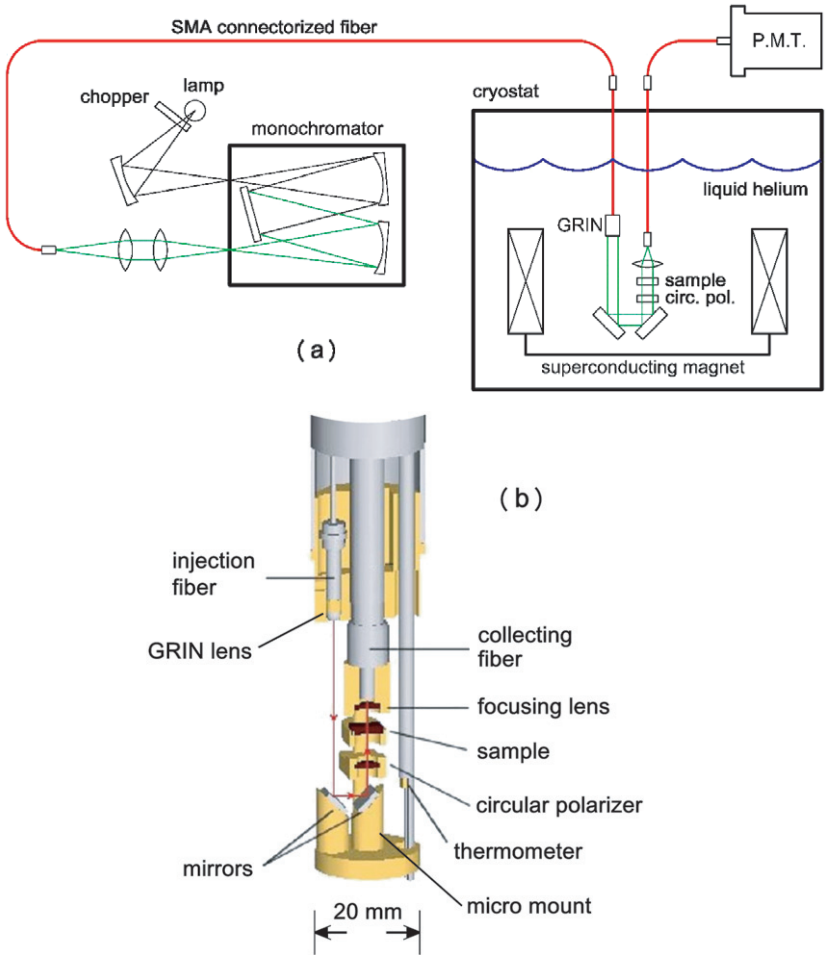

Figure 1. (a) Scheme of the experimental setup; (b) detail of the sample holder tip, drawn to scale. (This figure is in colour only in the electronic version)

coupling to the experimental apparatus, the optical fiber ends were connectorized using 'SMA' style connectors. The mirror below the sample was fixed on a micro mount, which allowed for XZ translation, rotation around a vertical axis, and tilt around a horizontal axis. The micro mount was used to move the mirror and steer the beam that went through the sample, to obtain optimal alignment and launching maximum light into the collecting fiber. The circular polarizer was home made and consisted of a linear polarizer on top of which a mica quarter wave plate at $\lambda = 589$ nm was fixed, with its fast axis aligned at 45° with the easy axis of the linear polarizer.

The absorption coefficient was obtained from the ratio of the transmission spectra with and without the sample. The magnetic field could be varied from 0 to 9.6 T. The σ^+ absorption spectrum was obtained when the magnetic field was parallel to the direction of light travel. To obtain the σ^- spectrum, the direction of the magnetic field was reversed. The measured spectra were not corrected for reflection losses at the surface of the sample and at the substrate/EuTe layer interface. Such a correction depends on the wavelength, because the EuTe index of refraction increases when the photon energy approaches the bandgap. Moreover,

at high fields when the sample is magnetized, optical activity is induced [12], hence the index of refraction is also dependent on the direction of circular polarization, meaning a different Fresnel transmission coefficient for each polarization. Therefore the reflection losses will be dependent on the wavelength, magnetic field, and direction of circular polarization. However, it is reasonable to assume that these reflection losses will increase smoothly as a function of the EuTe refractive index, which increases monotonically when the photon energy approaches the bandgap energy. Therefore, apart from a background monotonic contribution, reflection losses are not expected to influence the narrow absorption bands that are the focus of the present investigation, because these absorption bands are very well defined within a narrow energy range.

3. Theory

3.1. Spin domains as a function of magnetic field

In the molecular-field approximation [15], EuTe can be described by two sublattices, whose spin orientation will be determined by the minimum energy of the Hamiltonian

$$\mathcal{H} = \lambda M^2 \hat{M}_1 \cdot \hat{M}_2 - M(\hat{M}_1 + \hat{M}_2) \cdot \boldsymbol{B} + \mathcal{H}_a. \tag{1}$$

The first term represents the exchange interaction between the localized Eu^{2+} spins, where $\lambda = \frac{24|J_1+J_2|}{N g_S^2 \mu_B^2}$, J_1 and J_2 are the first and second neighbor exchange interaction constants, respectively, $N = 4/a^3$ is the density of Eu atoms in the lattice, $a = 6.598$ Å is the lattice constant of EuTe, $g_S = 2$ is the Eu^{2+} Landé gyromagnetic factor, $M = \frac{N}{2}\mu_B\sqrt{S(S+1)}$ is the saturation magnetization of each sublattice, and $\hat{M}_1$ and $\hat{M}_2$ are unit vectors in the direction of the sublattice magnetizations. The second term represents the Zeeman interaction of the Eu^{2+} spins, where the magnetic field intensity B is the internal field, which is smaller than the applied field due to the demagnetization effect [18] (see [17] for further details). $\mathcal{H}_a$ is the anisotropy energy density [16]:

$$\mathcal{H}_a = \frac{3K_1}{8}(\cos\theta_1 - \cos\theta_2)^2 - \frac{K_2}{2}\left(\sin^2 3\varphi_1 + \sin^2 3\varphi_2\right), \tag{2}$$

where θ_i and φ_i are the azimuth and zenith spherical coordinates, respectively, for the unit vectors $\hat{M}_i$, in a coordinate reference frame, in which the z-axis is along the hard axis (the [111] crystal direction) and the y-axis is along the easy axis, i.e., the $[11\bar{2}]$ crystal direction. Herewith we use values of $K_1 = 2.4 \times 10^5$ J m^{-3} and $K_2 = 40.1$ J m^{-3} in equation (2), which were taken from [16].

Since there are four equivalent [111] directions, equation (2) describes one of four so-called T-domains; within each T-domain, substitution of (2) into (1) shows that for $B = 0$ the minimum of equation (1) occurs when the arrangement is antiferromagnetic and $\hat{M}_i$ is parallel to any of three equivalent $[11\bar{2}]$ directions (hence there are three so-called S-domains). For $\boldsymbol{B}$ along the hard axis of a given T-domain, each S-domain generates a separate solution: the angle ϕ between $\hat{M}_i$ and $\boldsymbol{B}$ varies smoothly from $\phi = \pi/2$ to 0, according to

$$\cos\phi = \begin{cases} B/B_{sat} & \text{if } B < B_{sat} \\ 1 & \text{if } B > B_{sat}, \end{cases} \tag{3}$$

where

$$B_{sat} = 2\lambda M \tag{4}$$

is the saturation field. For other orientations of $\boldsymbol{B}$ relative to the hard axis, a numerical solution of equation (1) must be obtained. This was the required approach used in this work, because

in an arbitrary magnetic field the arrangement of the Eu^{2+} spins is described by a multiple domain structure, and not by a single spin domain of equation (3). At a field of approximately $B \sim 0.08$ T, a spin–flop transition occurs [16]. Since the spin–flop transition occurs at very low fields, when the absorption is effectively unchanged from its zero-field shape, no evidence of the spin–flop transition is observed in the absorption spectrum.

To describe the experimental data we choose λ based on the fact that the magnitude of the internal saturation field is well known, i.e. $B_{\rm sat} = 7.2$ T. Then λ can be deduced from equation (4), $\lambda = \frac{B_{\rm sat}}{2M} = 7.4 \times 10^{-6}$ T^2 m^3 J^{-1}, which is within the range of accepted values $\lambda = \frac{24|J_1+J_2|}{Ng_s^2\mu_B^2} = (7 \pm 1) \times 10^{-6}$ T^2 m^3 J^{-1}, where $J_1 = -0.43 \pm 0.001$ K, $J_2 = 0.15 \pm 0.01$ K is used [19].

3.2. Optical absorption of circularly polarized light

For an arbitrary orientation of the magnetic field vector $\boldsymbol{B}$, and of the wavevector $\boldsymbol{k}$ of circularly polarized light, the absorption will be given by [12][3]

$$\alpha(h\nu) = \sum_f \frac{\pi\, N\, h\nu\, e^2}{2\epsilon_0 \hbar c} \overline{|\boldsymbol{M}_f|^2} g(h\nu - E_f), \tag{5}$$

where $\boldsymbol{M}_f$ is the electric dipole matrix element between the initial state and a given final state, E_f is the energy of the excited state relative to the ground state, $g(h\nu)$ is a normalized lineshape function, whose width is a measure of the width of the narrow d-conduction band, and the bar represents the average over all Eu^{2+} spin orientations present in the sample, which can be obtained as described in the previous section 3.1.

In this work we studied optical absorption in the Faraday geometry, when $\boldsymbol{B} \parallel \boldsymbol{k}$. In our earlier work [12], we examined only the limit of very high magnetic fields, when the arrangement of the Eu^{2+} spins is ferromagnetic, and light interacts with a single ferromagnetic domain. In that case, the averaging in (5) could be omitted. What makes the calculations described in [12] especially simple is the fact that $\boldsymbol{B}$ and $\boldsymbol{k}$ were assumed parallel to the [001] direction. Under this condition, the quantization axis for the electronic angular momenta of the wavefunctions involved in the dipole matrix element (5) coincides with $\boldsymbol{k}$ and with the crystalline [001] direction, which simplifies the calculation of the matrix elements. Here, however, we are considering magnetic fields lower than the saturation value, and the spin order is not ferromagnetic, which makes calculation of the matrix elements much more complicated. For $B < B_{\rm sat}$, the sample is broken into a multiple domain structure. In order to calculate the absolute value of the absorption stemming from each magnetic domain, the wavefunctions contained in the matrix element in equation (5) must be brought to a common reference frame. The common reference frame chosen is one whose angular momentum quantization axis is along $\boldsymbol{k}$. The wavefunctions are moved into the common reference frame by rotations through Euler angles, using Wigner matrices [20]. A detailed description of this technical issue is left for publication elsewhere [21].

4. Results and discussion

Figure 2 shows the results of experimental measurements and of the calculations. The spectra shown in figure 2 were measured in the Faraday configuration, with incident light traveling normal to the sample surface, i.e., along the [111] crystalline direction. In order to investigate the absorption anisotropy, we also measured the absorption spectrum when the sample was

[3] Note that the number 2 appears in the denominator, instead of a typing error in [12].

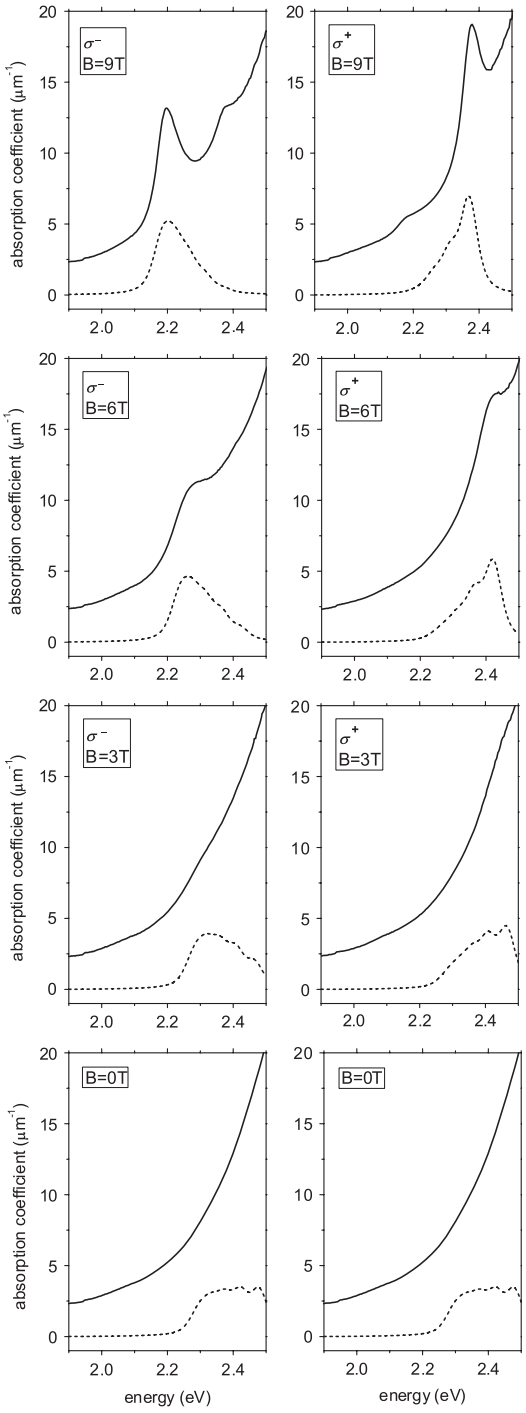

Figure 2. Experimental (solid curves) and theoretical (dashed curves) absorption of circularly polarized light in EuTe, in the Faraday configuration, for light traveling along the [111] crystalline direction. Curves labeled $\sigma^{\pm}$ correspond to the absorption of photons that possess an angular momentum with projection $\pm\hbar$ in the direction of the Eu^{2+} spins, when B is large and imposes ferromagnetic arrangement.

tilted, such that light traveled along the [001] crystalline direction, and the spectrum showed no obvious difference from the [111] spectrum. However, a rigorous quantitative comparison of the [111] and [001] spectra was not performed, because such a comparison would require to take into account complicated reflection losses described in section 2, which could be quite different in each case, due to the different angles of incidence.

At high fields, the absorption spectrum is strongly dichroic. For both polarizations, the spectrum is described by a single strong narrow absorption peak (width ∼50 meV) on top of a monotonically rising background absorption. The σ^- absorption maximum is seen at a photon energy of ∼2.2 eV, which is about 200 meV less than the position of the σ^+ maximum seen at ∼2.4 eV.

Figure 2 shows that a residuum of the strong peak seen in one circular polarization also appears as a much weaker peak in the absorption spectrum taken in the opposite circular polarization. No such residua were seen in the theoretical spectra. The experimental observation of residual peaks is a consequence of the non-ideality of the circular polarizer used. Instead of letting through a single circular polarization component, the non-ideal circular polarizer used in this work leaks a little light of the undesired opposite circular polarization component. The leakage is due to (a) the operation at wavelengths that deviate from the circular polarizer's nominal value and (b) a possible small misalignment of the linear polarizer easy axis from a direction at 45° to the fast axis of the $\lambda/4$ wave plate. Other effects, such as a possible deviation of the polarizer orientation from a horizontal position, will also contribute to circular polarization leakage. All these effects cause the output light from the nominally circular polarizer to be elliptically polarized. The elliptically polarized light can be described by a superposition of two circularly polarized components: one with a large intensity, circularly polarized in the desired direction, and another with a small intensity (leakage), with opposite circular polarization. Such a polarization leakage is the cause for the infiltration of the peak from one polarization spectrum into the other. For instance, in the region of the σ^- peak, when α^- is much greater than α^+, the absorption coefficient α^+ measured experimentally will be given by

$$\alpha^+\big|_{\text{measured}} = \frac{1}{d}\ln\frac{I_0^+ + \delta I_0^-}{I^+ + \delta I^-} = \frac{1}{d}\ln\frac{I_0^+ + \delta I_0^-}{I_0^+ \mathrm{e}^{-\alpha^+ d} + \delta I_0^- \mathrm{e}^{-\alpha^- d}} \approx \alpha^+ + \frac{\delta I_0^-}{I_0^+}\left(\alpha^- - \alpha^+\right), \quad (6)$$

where d is the sample thickness, I_0^+ and I^+ are intensities of the right-hand circularly polarized light entering and exiting the sample, respectively, δI_0^- is the intensity of left-hand circularly polarized light that leaks through the polarizer, and δI^- is what remains of it after passing through the sample. The approximate sign is valid if $\delta I_0^- \ll I_0^+$ and $(\alpha^- - \alpha^+)d \gg 1$.

Equation (6) shows that the height of the artificial peak that infiltrates from the σ^- into the σ^+ experimental spectrum will be approximately given by $\Delta\alpha^+ \approx (\delta I_0^-/I_0^+)\alpha^-$. Taking $\Delta\alpha^+ \sim 0.5\ \mu\mathrm{m}^{-1}$ and $\alpha^- \sim 15\ \mu\mathrm{m}^{-1}$ (see figure 2), then $(\delta I_0^-/I_0^+) \sim 3\%$ is found.

Notice also in figure 2 that the height of the infiltrated peak seen in the σ^- spectrum is slightly larger than in the σ^+ one, indicating a slightly larger polarization leakage at the photon energy of 2.4 eV ($\lambda = 517$ nm) than at 2.2 eV ($\lambda = 546$ nm). A larger leakage at $\lambda = 517$ nm than at $\lambda = 564$ nm is indeed expected, because in the former case the photon wavelength deviates much more from the nominal wavelength of the circular polarizer used in this work (589 nm, see section 2) than in the latter case.

Theoretical absorption spectra were calculated using the prescription given in section 3.2. The theoretical spectra for light propagating along the [111] direction are shown in figure 2. For other crystalline directions the theoretical absorption spectra showed only a small difference from the [111] spectrum, in agreement with experiment. The high-field theoretical spectra shown in figure 2 are slightly different from those published in [12], because in [12] (a) light

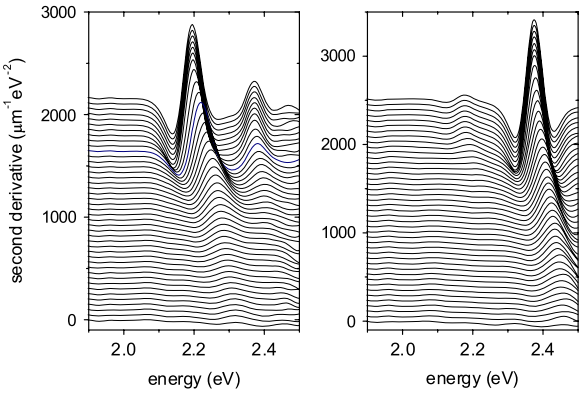

Figure 3. Second derivatives of the σ^- (left panel) and σ^+ (right panel) of the experimental absorption spectra of EuTe, taken at regular magnetic field intervals. The lowest curve corresponds to $B = 0$ and the uppermost curve to $B = 9.6$ T.

was assumed to travel along [001] and (b) the broadening function was a Gaussian with full width at half maximum of 50 meV, whereas here a Voigtian was used, with a larger width of 60 meV (a justification for this choice of broadening is discussed below). Figure 2 shows that the dichroic doublet seen in the experimental spectra at high fields is well reproduced by the theory, except for the monotonically rising background, which is evidence of the existence of electronic states other than the $5d(t_{2g})$ conduction band, which were not included in the theoretical model.

As the field is decreased, the absorption edge blue shifts, due to the well known d–f exchange interaction described by Wachter [19]. The functional dependence of the absorption peak positions on the magnetic field is given in [17]. On decreasing the field, the doublet structure becomes weaker and less resolved, both in the experimental and in the theoretical spectra. At $B = 0$ only a very weak structure remains in the theoretical absorption spectrum, described by a broad absorption background. In the experimental spectrum, no such obvious similar structure is seen at $B = 0$, and this is due to the presence of a strong monotonic absorption background. By double differentiating the spectrum, the monotonic background can be removed, and the second derivatives of the experimental absorption spectra are shown in figure 3. Figure 3 demonstrates that indeed there is some remaining modulation of the absorption coefficient even at $B = 0$, although it is two orders of magnitude weaker than at high fields. The slightly stronger amplitude modulation seen in the theoretical spectra at $B = 0$, in comparison with the experimental ones, can be attributed to the residual spin–orbit interaction within the $5d(t_{2g})$ conduction band, not included in the theory, which leads to a weaker modulation of the density of states, due to the additional broadening of the energy levels.

The parameters entering the theoretical calculations are λ_{4f}, $J_{df}S$, E_G, r_{df}, and the energy width of the broadening function $g(h\nu)$ in equation (5). The 4f spin–orbit interaction constant, $\lambda_{4f} = 9.6$ meV, is deduced from the splitting between the σ^- and σ^+ absorption peaks at $B = 0$ [12]). In our previous investigation [17], parameters $J_{df}S = 0.15$ eV and $E_G = 2.321$ eV (the EuTe gap) were deduced from the total redshift of the σ^- absorption band [17]. This deduction was made assuming that the redshift of both the σ^- and the σ^+ bands was identical to the redshift of the seven individual lines that compose them, and which arise because of the Landé splitting of the $4f^6(^7F_J)$ core state ($J = 0, \ldots, 6$). However, even if we assume that all seven lines shift rigidly by the same fixed amount when the magnetic

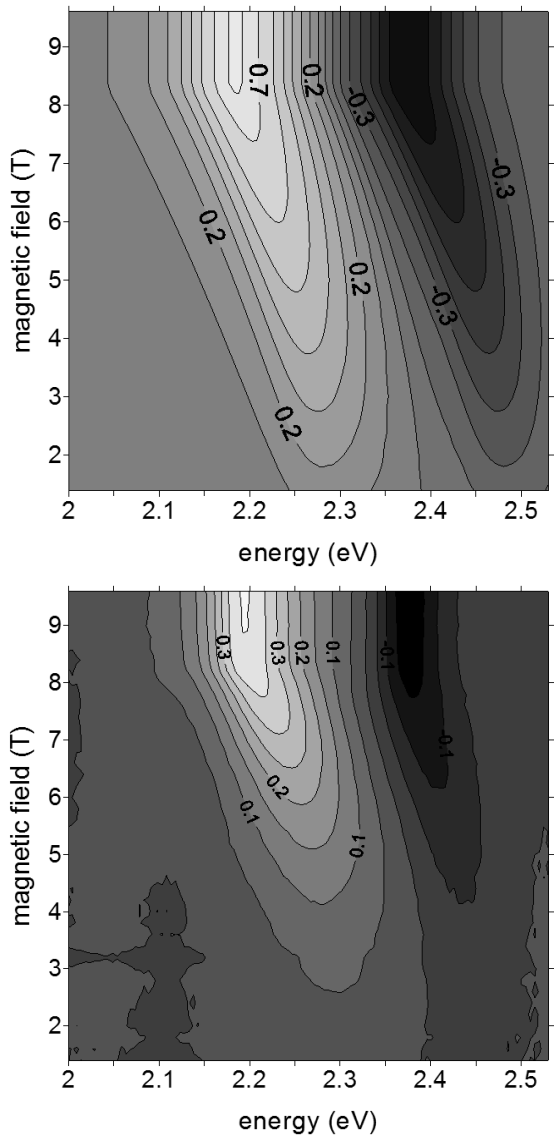

Figure 4. Contour plots of the experimental (lower panel) and theoretical (upper panel) magnetic circular dichroism in EuTe.

field increases, their envelope functions σ^+ and σ^- will not display the same energy shift. This is because the contribution to the envelope function stemming from each individual line is proportional to the oscillator strength of the associated electronic transition. However, the oscillator strength dependence on the magnetic field intensity is very different for each line. As a result of this, the total energy shifts of the σ^+ and σ^- envelopes turn out different from one another. More specifically, when B increases, the oscillator strength for σ^- transitions increases much more for low J values than for large values of J, and therefore the total redshift of the σ^- absorption band is greater than $J_{\mathrm{df}}S$, i.e., it is greater than the total redshift of the individual lines. For the σ^+ transitions the opposite is true, hence the redshift of the

σ^+ absorption band is smaller than $J_{\rm df}S$. (This is in agreement with the experiment: figure 3 clearly shows that the redshift of the σ^- absorption band is greater than that of the σ^+ one.) Taking this into consideration, a better estimate of $J_{\rm df}S$ than that used in [17] is the average redshift of the σ^- and σ^+ lines. Using the redshift values for the σ^- and σ^+ lines obtained in [12], we deduce $J_{\rm df}S = 0.11$ eV and this is the parameter value used herewith. The 4f–5d overlap integral was taken to be $r_{\rm df} = 0.18$ Å. Finally, for $g(h\nu)$ we used a Voigt broadening function, which better describes the slowly increasing sidebands in the experimental absorption than the much more abrupt Gaussian lineshape used in our previous analysis of the high-field spectrum [12]. The Voigtian function was obtained as a convolution of a Lorentzian and a Gaussian, with equal full widths at half maximum of 0.06 eV. This value represents an estimate of the energy width of the 5d(t_{2g}) conduction band in EuTe.

As an additional test of the model, we measured and calculated the magnetic circular dichroism (MCD) of the absorption coefficient as a function of photon energy and magnetic field intensity, which is defined by

$$\text{MCD} = \frac{\alpha^- - \alpha^+}{\alpha^- + \alpha^+},$$

where $\alpha^{\pm}$ is the absorption coefficient for σ^+ and σ^- geometries. The experimental and theoretical MCD spectra, as a function of photon energy and external magnetic field, are shown in a contour plot in the lower and upper panels of figure 4, respectively. At $B = 0$ (not shown in figure 4), MCD $= 0$, because of the symmetry of the antiferromagnetic arrangement. The qualitative agreement between theory and experiment is good; however, the absolute values of theoretical MCD are larger than the experimental ones, and the discrepancy increases with the photon energy. This discrepancy is due to the monotonically rising absorption background seen experimentally, which is not accounted for in the theory used here.

In conclusion, the absorption magnetic circular dichroism in EuTe was investigated as a continuous function of the magnetic field intensity at $T = 2$ K. The experimental results were analyzed within a theoretical model that takes into account the arrangement of the Eu^{2+} spins in the crystal lattice. The dramatic changes of the absorption spectrum as a function of field can be well explained by the complex dependence of the Eu^{2+} spin domain ensemble on the magnetic field intensity.

Acknowledgments

ABH acknowledges financial support provided by CNPq (project 308116/2004-6). BLD also acknowledges support from CNPq.

References

[1] Zutic I, Fabian J and Sarma S D 2004 *Rev. Mod. Phys.* **76** 323
[2] MacDonald A H, Schiffer P and Samarth A 2005 *Nat. Mater.* **4** 195
[3] Greilich A, Yakovlev D R, Shabaev A, Efros A L, Yugova I A, Oulton R, Reuter V S D, Wieck A and Bayer M 2006 *Science* **313** 341
[4] Datta S and Das B 1990 *Appl. Phys. Lett.* **56** 665
[5] Dimmock J O 1970 *IBM J. Res. Dev.* **14** 301
[6] Santos T S and Moodera J S 2004 *Phys. Rev.* B **69** 241203(R)
[7] Guntherodt G, Wachter P and Imboden D M 1971 *Phys. Kondens. Mater.* **12** 292
[8] Guntherodt G, Wachter P and Imboden D M 1974 *Phys. Condens. Matter.* **18** 37
[9] Sakai O, Yanase A and Kasuya T 1977 *J. Phys. Soc. Japan* **42** 596
[10] Reim W and Schoenes J 1990 *Ferromagnetic Materials* vol 5 (Amsterdam: North-Holland) p 183
[11] Mauger A and Godart C 1986 *Phys. Rep.* **141** 51

[12] Henriques A B, Wierts A, Manfrini M A, Springholz G, Rappl P H O, Abramof E and Ueta A Y 2005 *Phys. Rev.* B **72** 155337
[13] Henriques A B, Galgano G D, Díaz B, Rappl P H O and Abramof E 2007 *Proc. 28th Int. Conf. on the Physics of Semiconductors*; *AIP Conf. Proc.* **893** 1233
[14] Henriques A B, Manfrini M A, Galgano G D, Díaz B L, Rappl P H O and Abramof E 2007 *Int. J. Mod. Phys.* B **21** 1247
[15] Smart J S 1966 *Effective Field Theories of Magnetism* (London: Saunders)
[16] Battles J W and Everett G E 1970 *Phys. Rev.* B **1** 3021
[17] Henriques A B, Hanamoto L K, Oliveira N F, Rappl P H O, Abramof E and Ueta A Y 2004 *J. Phys.: Condens. Matter* **16** 5597
[18] Blundell S 2001 *Magnetism in Condensed Matter* (Oxford: Oxford University Press) appendix D
[19] Wachter P 1979 *Handbook on the Physics and Chemistry of Rare Earth* vol 1 (Amsterdam: North-Holland) p 507
[20] Landau L D and Lifshitz E M 1974 *Kvantovaya Mehanika* (Moscow: Nauka)
[21] Henriques A B, Manfrini M A, Abramof E and Rappl P H O 2007 in preparation